Journal of Biomedical Optics

BiomedicalOptics.SPIEDigitalLibrary.org

# Test–retest reliability of brain mitochondrial cytochrome-c-oxidase assessed by functional near-infrared spectroscopy

Lisa Holper
J. John Mann

SPIE.

Lisa Holper, J. John Mann, "Test–retest reliability of brain mitochondrial cytochrome-c-oxidase assessed by functional near-infrared spectroscopy," *J. Biomed. Opt.* **23**(5), 056006 (2018), doi: 10.1117/1.JBO.23.5.056006.

# Test–retest reliability of brain mitochondrial cytochrome-c-oxidase assessed by functional near-infrared spectroscopy

**Lisa Holper*** **and J. John Mann**
Columbia University, New York State Psychiatric Institute, Division of Molecular Imaging and Neuropathology, New York, New York, United States

**Abstract.** Functional near-infrared spectroscopy (fNIRS) is a noninvasive method for measuring *in vivo* both hemodynamic and mitochondrial metabolic activities in brain cortical structures. Although the test–retest reliability of the hemodynamic measures, such as reflected by oxygenated ($HbO_2$), deoxygenated (HHb) hemoglobin, and the tissue oxygenation index (TOI), has been previously reported to be good to excellent, the reliability of the metabolic signal indexed by oxidized cytochrome-c-oxidase (oxCCO) has not been reported. The present test–retest study compared the reliability of the metabolic and hemodynamic signals in 10 healthy participants undergoing hypo- and hypercapnia challenges. The primary reliability measure was the intraclass correlation coefficient (ICC). Results of both hypo- and hypercapnia showed that the oxCCO signal (ICC = 0.876/0.757) had robust reliability comparable with that of the $HbO_2$ (ICC = 0.841/0.801), HHb (ICC = 0.804/0.571), and TOI (ICC = 0.574/0.614) signals. These findings show that the oxCCO signal can be assessed by fNIRS with comparable reliability to the hemodynamic measures. We discuss the results in light of current interest in a mitochondrial metabolic marker derived from fNIRS. *© 2018 Society of Photo-Optical Instrumentation Engineers (SPIE)* [DOI: 10.1117/1.JBO.23.5.056006]

Keywords: cytochrome-c-oxidase; reliability; near-infrared spectroscopy.

Paper 170797RR received Dec. 8, 2017; accepted for publication Apr. 24, 2018; published online May 15, 2018.

## 1 Introduction

Functional near-infrared spectroscopy (fNIRS) is an optical brain imaging method that has become a valuable neuroimaging technique in research and clinical settings.[1–4] The reliability of fNIRS hemodynamic measures is good to excellent (for review see Ref. 5). Test–retest performance has been examined in different conditions and age groups. Visual stimulation and finger-tapping measured over the occipital[6] and motor cortex[7] in healthy adults have been reported to have intraclass correlation coefficients (ICC) of 0.84 and 0.80, respectively. Rhythmic handgrip exercises measured over prefrontal lobe revealed similar reliability in healthy adults (ICC = 0.83) compared with patients with moderate to severe traumatic brain injury (ICC = 0.70).[8] Functional brain networks during resting-state investigated using independent component analysis[9] and graph metrics[10] have been reported to exhibit fair (ICC = 0.56) to good (0.6 < ICC < 0.74) reliability, respectively. Excellent reliability (ICC = 0.89 to 0.94) has been shown in infants of ages 4 to 16 months during visual-auditory recordings.[11] Studies of peripheral muscle in healthy adults during handgrip contraction found ICC = 0.86,[12] and in patients with chronic heart failure during leg muscle cycling, ICC = 0.85 to 0.92.[13]

In addition to the hemodynamic measures based on the two primary chromophores, i.e., oxygenated ($HbO_2$) and deoxygenated (HHb) hemoglobin (as assessed using wavelengths around 775 and 850 nm, respectively), fNIRS is also capable of monitoring a third chromophore, which is the mitochondrial cytochrome-c-oxidase (CCO), assessed using a wavelength around 810 nm (Fig. 1) (for review see Ref. 14). The optical signature of the CCO is predominantly the $Cu_A$ center, which is the binuclear copper site in soluble domains of CCO. fNIRS measures the oxidation state of mitochondrial CCO, termed oxCCO signal, which is an indicator of the CCO redox changes. CCO is the terminal electron acceptor in the mitochondrial respiratory chain and joint responsible for over 95% of the oxygen metabolism in the synthesis of adenosine triphosphate,[15] the main source of cellular energy. The *in vivo* concentration of oxCCO is ~10% that of hemoglobin, making it harder to detect.[16] Yet, despite its small change in amplitude, the oxCCO signal is a remarkably stable signal,[14] and has a higher brain-specificity compared with hemoglobin.[17–19] While the hemoglobin measures, $HbO_2$ and HHb, provide information on hemodynamic circulation and intravascular oxygenation, oxCCO is an indicator of cellular oxygen metabolism.[20–23] Changes in oxCCO indicate an alteration in the balance between oxygen delivery and oxygen consumption.[24] Hence, a more complete analysis of cerebral health requires concurrent monitoring of all three chromophores. Applications of this approach included assessment of neonatal brain injury[16] or traumatic brain injury,[25,26] bedside monitoring of cortical mitochondrial metabolic status in clinical settings,[22,23,27] or the assessment of cognitive tasks, such as driving.[28] These brain mitochondrial functions cannot be assessed using other neuroimaging methods, such as functional magnetic resonance imaging (fMRI).

Unlike the hemodynamic measures, the reliability of oxCCO measurements has so far not been reported. Reasons for this may be because it is harder to detect and requires special fNIRS instrumentation[14,16,18] that is currently commercially not available.

*Address all correspondence to: Lisa Holper, E-mail: holper@ini.phys.ethz.ch

1083-3668/2018/$25.00 © 2018 SPIE

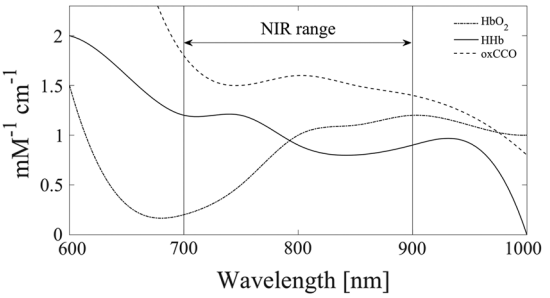


**Fig. 1** Chromophores absorption spectra. Spectra for the three chromophores, $HbO_2$ (as assessed using wavelengths around 775 nm), HHb (around 850 nm), and oxCCO (around 810 nm), present in human tissue that can be measured using fNIRS in the near-infrared (NIR) range from 700 to 900 nm. The spectra are specified with respect to their specific concentration in mM.

In the present study, we therefore aimed to test–retest the oxCCO signal and to provide a first estimate of its reliability in a healthy population.

## 2 Materials and Methods

### 2.1 *Participants*

Ten physically and psychiatrically healthy adult volunteers [six females, mean age $(\pm\text{STD}) = 34 \pm 4.5$ years] were recruited by advertising and posted flyers. Exclusion criteria were any psychiatric, or neurological disorder, unstable medical condition, or pregnancy. All participants gave written informed consent. The study was approved by the Institutional Review Board of the New York State Psychiatry Institute and performed in accordance with the Declaration of Helsinki.

### 2.2 *Respiratory Challenges*

Quantification of the oxCCO signal demands significant changes in the arterial oxygen saturation to be reliably detected in the cortex. Therefore, two respiratory challenges were chosen as previously described[29] to systemically manipulate cerebral oxygenation via hypo- and hypercapnia, i.e., reduced and increased carbon dioxide in the blood. For the test–retest design, data from each participant were collected in two sessions at the same time of the day separated by one week. In each session, participants underwent both challenges.

***Hypocapnia*** was induced by hyperventilation consisting of five repetitions of alternate periods of rapidly breathing in and out with constant respiratory volume (20 s) and normal breathing (40 s) with a total duration of five minutes.

***Hypercapnia*** was induced by breath-holding consisting of five repetitions of alternate periods of breath hold (20 s) and normal breathing (40 s) with a total duration of five minutes. Participants were trained prior to recording to perform the inspirational breath-hold volume of air similar to a normal breath cycle to avoid inhaling larger volumes of air than the volume of a normal breath cycle.

Prior to and after each challenge, a resting-state of five minutes was collected, during which participants were asked to sit still with their eyes open to allow the hemodynamic cortical system to normalize. The resting-state periods were not included in the retest analysis.

### 2.3 *Functional Near-Infrared Spectroscopy Instrumentation*

An NIRO 300 instrument (Hamamatsu Photonics) was used to collect simultaneous measurements of the metabolic and hemodynamic fNIRS signals. The instrument delivers four wavelengths of light (775, 810, 850, and 910 nm, respectively, Fig. 1) by four light sources (pulsed laser diodes) that are detected by three closely placed detectors (photodiodes) (Fig. 2). The concentration changes of oxCCO, $HbO_2$, and HHb are measured by conventional differential spectroscopy with the use of a modified Beer–Lambert law.[30,31] In addition, the system measures the tissue oxygenation index (TOI) that is calculated based on the principle of spatially resolved reflectance spectroscopy.[30,32]

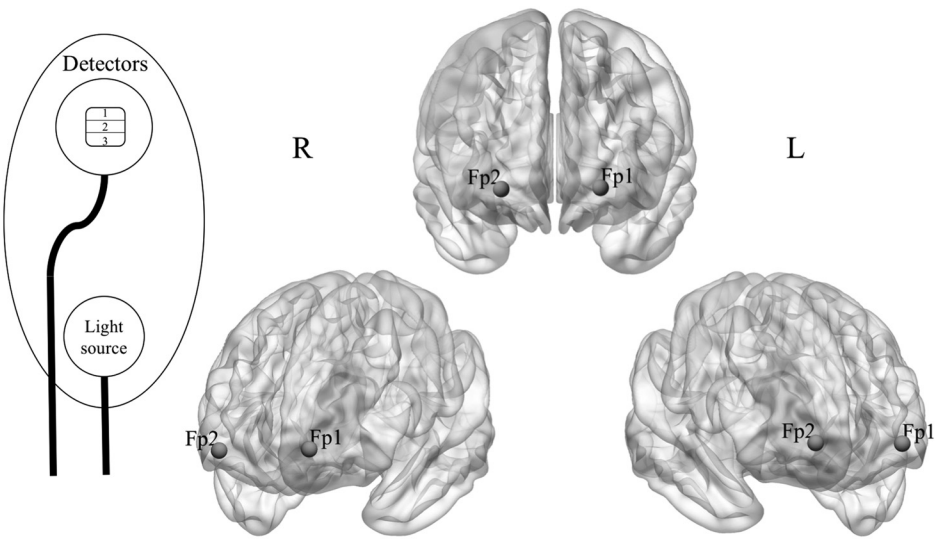


**Fig. 2** (Left) NIRO 300 sensor. The light sources and detectors ($\sim 10 \times 10$ mm$^2$) were held in a light proof holder and set at a distance of 4.5 cm. Concentration changes of oxCCO, $HbO_2$, and HHb were measured by the middle photodiode, whereas TOI is measured by the use of all three. (Right) fNIRS setup. Illustration of the probe positioning of the NIRO 300 (Hamamatsu Photonics). Areas of the dorsolateral prefrontal cortex were identified using the Montreal Neurological Institute (MNI) space brain atlas converted to the International 10–20 System.

TOI can be approximated as the ratio of oxygenated to total tissue hemoglobin. The oxCCO, $HbO_2$, and HHb concentration changes are measured by the middle photodiode, whereas TOI is measured by the use of all three. The light sources and detectors ($\sim 10 * 10$ mm$^2$) were held in a light proof holder and set at a distance of 4.5 cm. Both light sources and detectors were fixed in a rubber probe to allow for direct skin contact. A fiberoptic plate was used as the detector window, allowing light to be conducted from the skin surface to the sensors without distorting the spatial distribution. Placed under a flexible head cap, two channels were positioned to cover parts of the dorsolateral prefrontal cortex (i.e., Fp1 and Fp2 according to the International 10–20 system[33]) (Fig. 2). Sampling rate was set to 1 Hz. Data were detrended, zero-meaned, and band-pass-filtered in the range 0.005 to 0.3 Hz, using a fifth-order Butterworth filter, to remove physiological noise, using functions of the HOMER2 processing package.[34]

Peripheral physiological measures were assessed using a capnometer (LifeSense LS1-9R, Nonin Medical) by means of the arterial tissue oxygen saturation ($SpO_2$) and the partial end-tidal carbon dioxide ($PetCO_2$) of the exhaled air. Participants wore a nasal cannula through which tidal gases were sampled at 1 Hz.

## 3 Data Analysis

All data analysis was performed using MATLAB® (Release 2017b, MathWorks, Massachusetts).

fNIRS data from both channels were averaged. Changes of the concentration of ΔoxCCO, ΔTOI, $\Delta HbO_2$, and ΔHHb were used as indicators of metabolic and hemodynamic activities.[1,7,11] The five hypo- and hypercapnia intervals were block-averaged and relative concentration changes were computed from the end of the rest period (i.e., time-locked two seconds before onset of hypo-/hypercapnia) to the end of the challenge period (i.e., time-locked two seconds after offset of hypo-/hypercapnia). The subject-specific signal changes were then used for the reliability analysis.

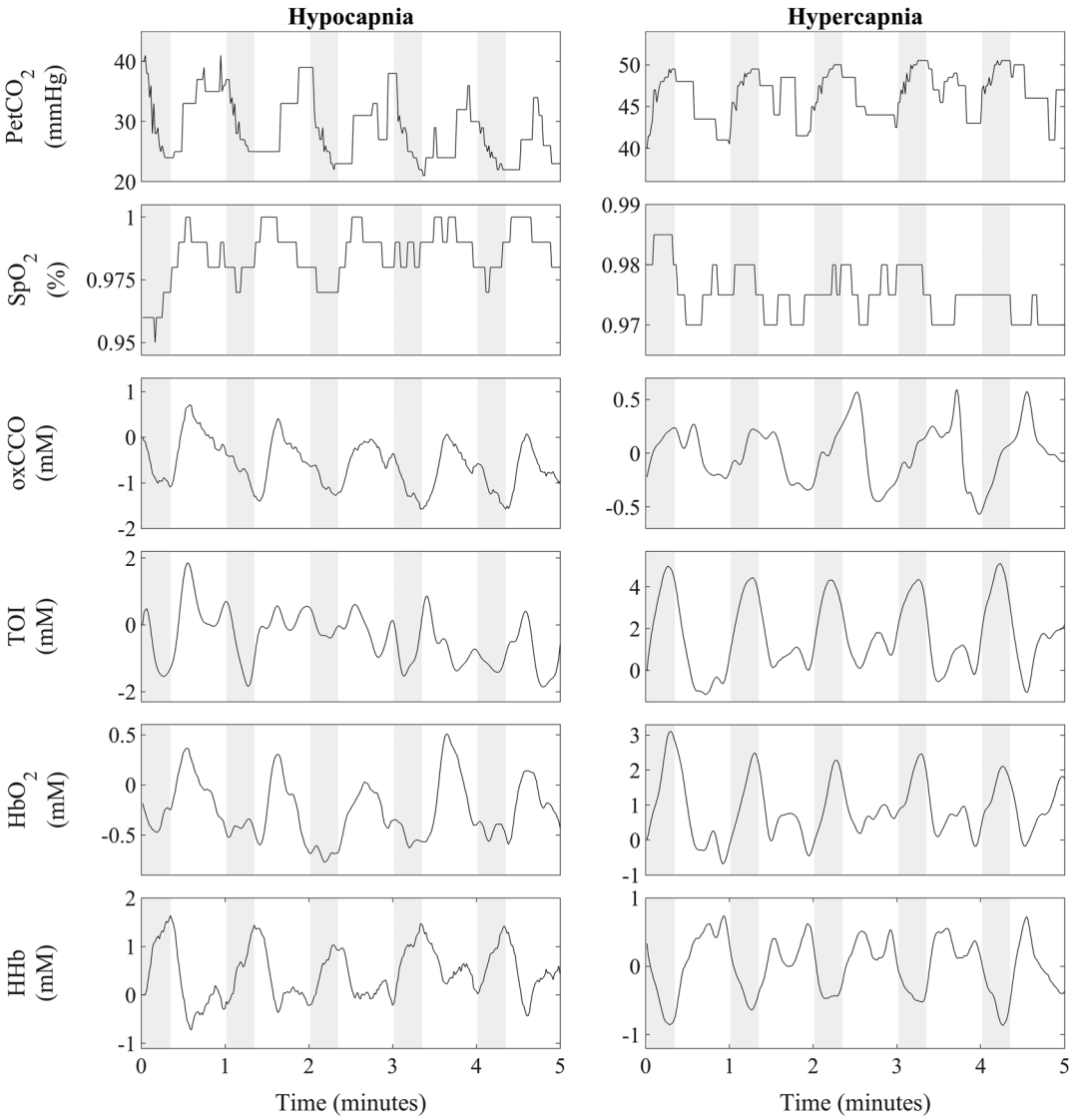


**Fig. 3** Measured signals. Experimentally measured peripheral physiological signals ($PetCO_2$, $SpO_2$) and fNIRS signals (oxCCO, TOI, $HbO_2$, and HHb, baseline corrected) are indicated by black lines. Gray patches indicate the hypo- and hypercapnia intervals (20 s) alternating with rest periods of normal breathing (40 s). Data are shown for an example participant.

### 3.1 *Reliability*

As primary measure of test–retest reliability, the ICC was applied using the following previous recommendations:[5]

- ICC was computed as type "3–1" according to the Shrout and Fleiss convention,[35] i.e., a two-way mixed single measures.
- The two-way mixed model was chosen based on the assumption that the results may not be generalized to fNIRS instruments other than the NIRO 300 (since currently commercially not available). The type of single measures was chosen because only the NIRO 300 instrument was used.
- ICC was calculated with confidence intervals based on an alpha level of significance $p < 0.05$. The corresponding $p$-value of a hypothesis test with the null hypothesis ICC $= 0$ was reported.
- Following the guidelines for interpretation by Cicchetti,[36] the ranges of ICC < 0.40, ICC 0.40 to 0.59, ICC 0.60 to 0.74, and ICC > 0.75, were considered to reflect poor, fair, good, and excellent test–retest reliability, respectively.

### 3.2 *Agreement*

As measure of agreement, Bland–Altman plots[37–39] were applied, which are based on the analysis of the differences between two measurements. Agreement quantifies how close two measurements made on the same subject are and is given in unit scale as the measurements themselves.[40] The corresponding estimates of agreement, i.e., mean difference, with lower and upper 95% limits of agreement (LoA), help in interpretation of the ICC[41] in that they uncover trends or consistent bias between measurement sessions.

### 3.3 *Repeatability*

Bland–Altman plots can also be used to assess the repeatability of a measure. The plot is then used to check whether the variability or precision is related to the size of the characteristic signal being measured. Optimally, for repeated measurements of the same instrument, the mean difference should be zero. Therefore, the coefficient of repeatability (CR) can be derived as two times the standard deviation of the differences between the two measurements.[37]

As the CR is a measure in the same unit scale as the measurements themselves, the coefficient of variation (CV) was calculated as an additional measure of dispersion expressed in percentage (%). The CV is defined as the ratio of the standard deviation to the absolute value of the mean.

## 4 Results

The experimentally measured signals from an example participant are shown in Fig. 3. The peripheral physiological data

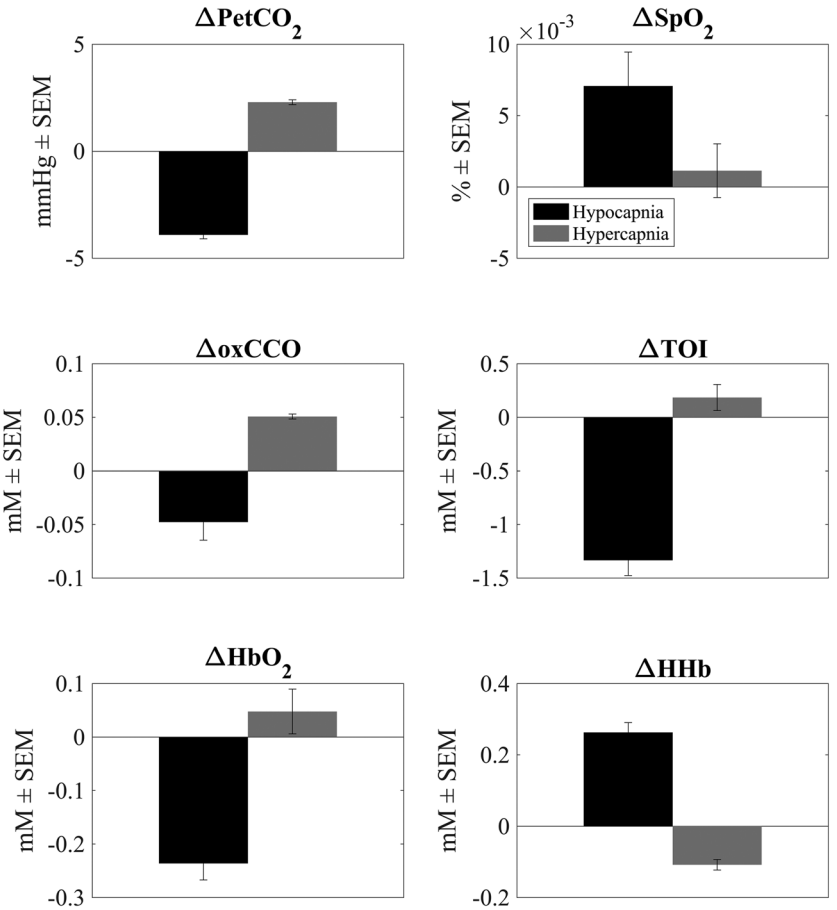


**Fig. 4** Signal changes. Block-averaged signal changes across all participants of the peripheral physiological measures ($\Delta PetCO_2$, $\Delta SpO_2$) and fNIRS data (ΔoxCCO, ΔTOI, $\Delta HbO_2$, and ΔHHb) for hypocapnia (black) and hypercapnia (gray). Error bars indicate the standard error of the mean (±SEM). There were no significant differences "between sessions" as assessed using ANOVA.

$PetCO_2$ and $SpO_2$, as well as the fNIRS data oxCCO, TOI, $HbO_2$, and HHb, are illustrated over the time course of the five hypo- and hypercapnia intervals (gray patches). All signals showed a relative change in response to hypo- and hypercapnia and a return close to baseline values after each challenge.

The block-averaged signal changes "across sessions" reflected typical responses to hypo- and hypercapnia (Fig. 4). Both the time courses as well as the relative magnitudes of the oxCCO, ΔTOI, $\Delta HbO_2$, and ΔHHb signals obtained during the respiratory challenges are in agreement with previous work.[19,28] In response to hypocapnia, we observed a decrease in $\Delta PetCO_2$ and an increase in $\Delta SpO_2$, whereas the fNIRS data showed a decrease in ΔoxCCO, ΔTOI, $\Delta HbO_2$, and an increase in ΔHHb. The opposite pattern was observed in response to hypercapnia, an increase in $\Delta PetCO_2$, a decrease in $\Delta SpO_2$, an increase in ΔoxCCO, ΔTOI, $\Delta HbO_2$, and a decrease in ΔHHb.

Importantly, there were no significant differences between sessions for any of the signals as assessed using ANOVA (one-way main effects of "session": hypocapnia $\Delta PetCO_2$ $F = 1.102$, $p = 0.307$; hypercapnia $\Delta PetCO_2$ $F = 0.798$, $p = 0.383$; hypocapnia $\Delta SpO_2$ $F = 2.037$, $p = 0.171$; hypercapnia $\Delta SpO_2$ $F = 0.466$, $p = 0.503$; hypocapnia ΔoxCCO $F = 0.418$, $p = 0.526$; hypercapnia ΔoxCCO $F = 0.001$, $p = 0.967$; hypocapnia ΔTOI $F = 1.346$, $p = 0.261$; hypercapnia ΔTOI $F = 0.018$, $p = 0.893$; hypocapnia $\Delta HbO_2$ $F = 3.366$, $p = 0.083$; hypercapnia $\Delta HbO_2$ $F = 1.367$, $p = 0.257$; hypocapnia ΔHHb $F = 0.657$, $p = 0.428$; hypercapnia ΔHHb $F = 1.036$, $p = 0.332$). The nonsignificance between sessions is considered to be an important aspect for ICC selection as it helps in determining the selection between one- or two-way models.[5]

The subject-specific signal changes were then used to estimate the reliability between sessions (Figs. 5 and 6, Table 1).

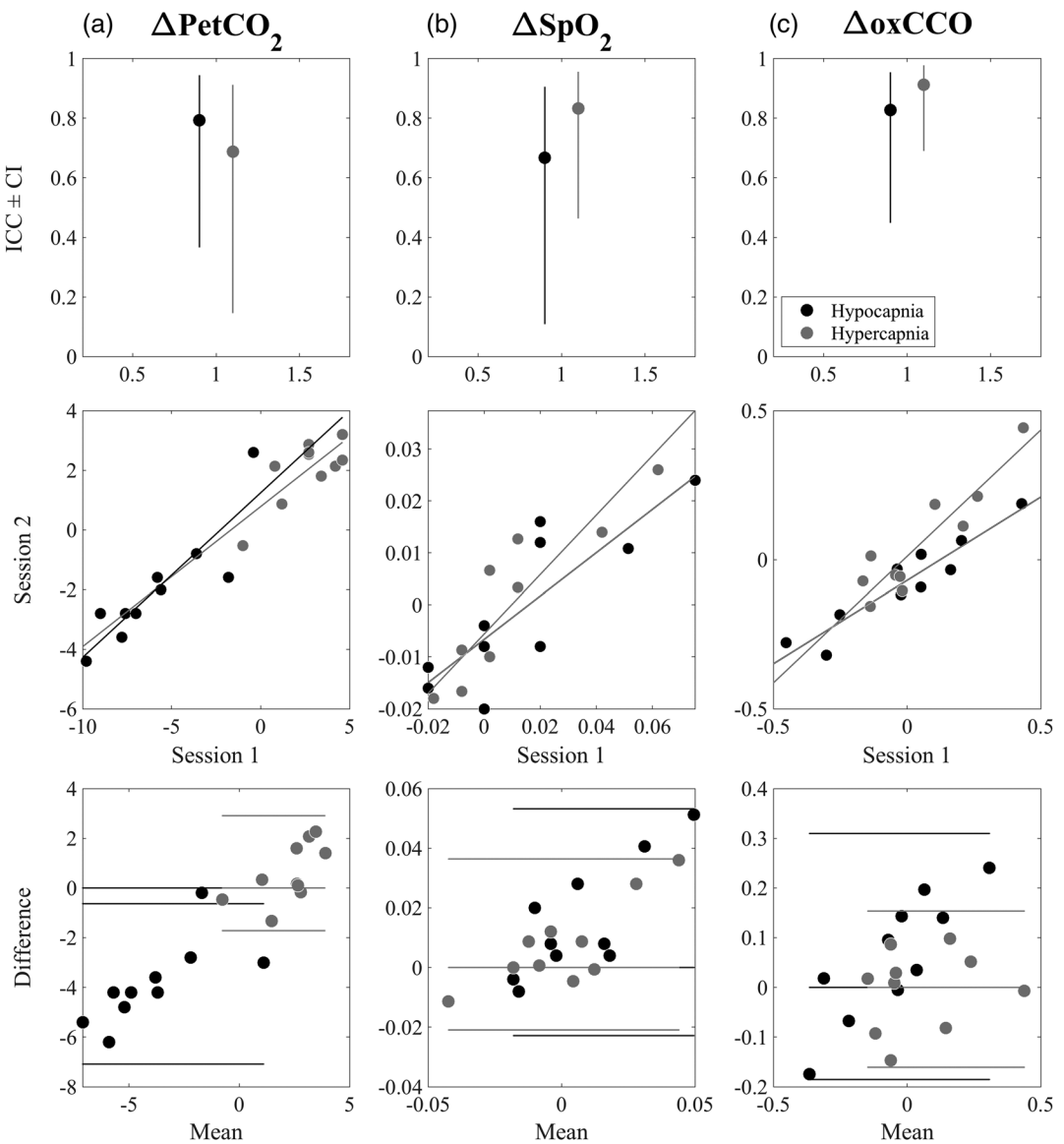


**Fig. 5** Reliability, agreement, and repeatability $PetCO_2$, $SpO_2$, and oxCCO. (a) ICCs (±CI) and (b) scatter plots illustrating the reliability between sessions. (c) Bland–Altman plots illustrating the agreement and repeatability between sessions as assessed by the mean differences. Data are shown for both hypocapnia (black) and hypercapnia (gray). See Table 1 for statistics.

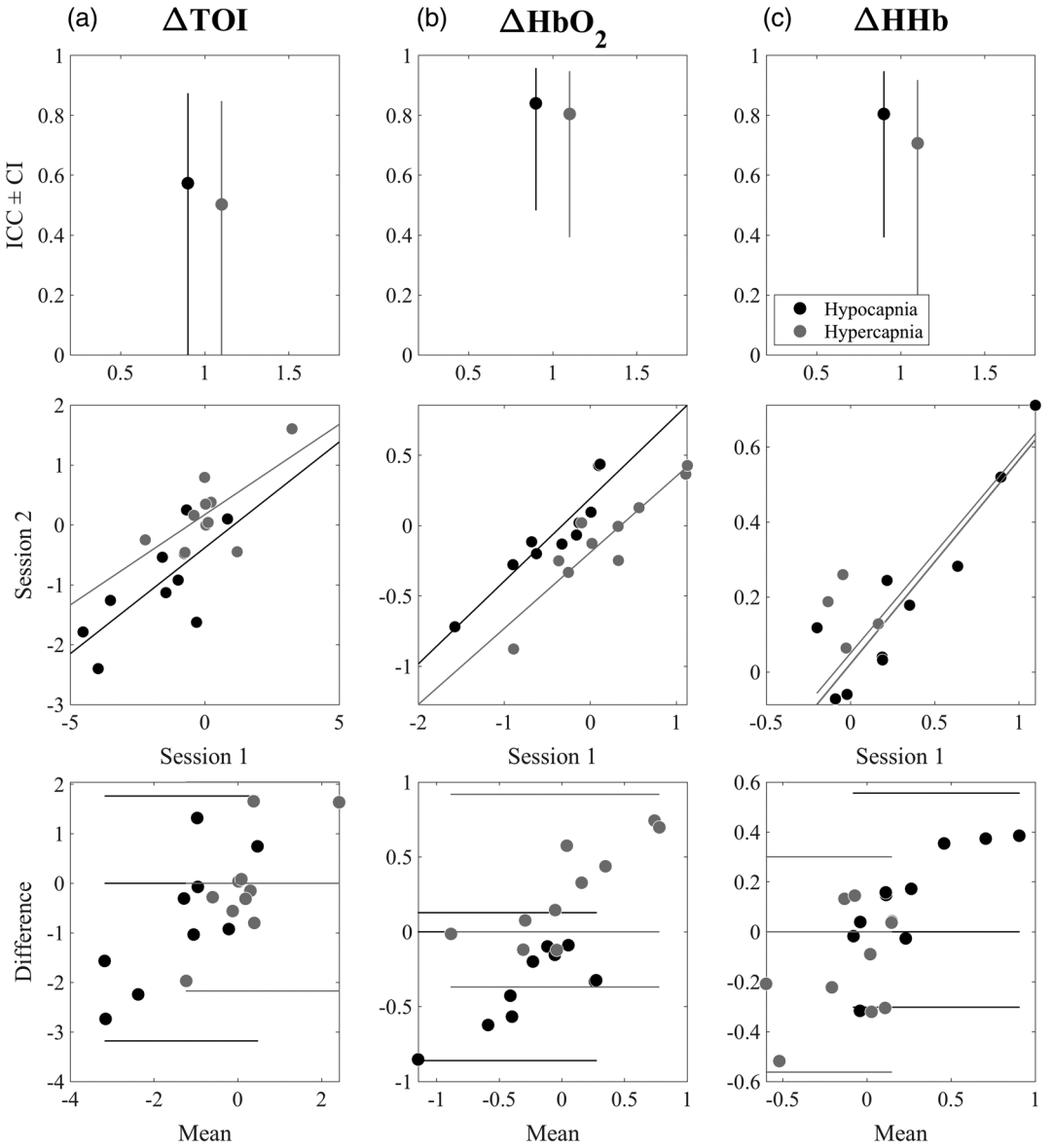


**Fig. 6** Reliability, agreement, and repeatability TOI, $HbO_2$, and HHb. (a) ICCs (±CI) and (b) scatter plots illustrating the reliability between sessions. (c) Bland–Altman plots illustrating the agreement and repeatability between sessions as assessed by the mean differences. Data are shown for both hypocapnia (black) and hypercapnia (gray). See Table 1 for statistics.

ICCs demonstrated good to excellent reliability for the peripheral measures $\Delta PetCO_2$ (hypo-/hypercapnia ICC = 0.518/745) and $\Delta SpO_2$ (ICC = 0.871/937). The NIRS data exhibited excellent reliability in all signals ΔoxCCO (ICC = 0.933/876), ΔTOI (ICC = 0.735/922), $\Delta HbO_2$ (ICC = 0.930/905), and ΔHHb (ICC = 0.916/579) as illustrated in the scatter plots.

In accordance, Bland–Altman plots demonstrated good agreement for all signals without significant differences in the mean differences as assessed using ANOVA. The evenly scattered measurement points without trends suggested that there was no consistent bias between sessions (Figs. 5 and 6). The mean differences were smaller for the oxCCO signal compared with the hemodynamic signals (Table 1) indicating that the metabolic measurements separated by a week were closer.

Repeatability refers to the variation in a measure under identical conditions over which the underlying signal can be considered to be constant.[40] Under such conditions, variability may then be ascribed to the measurement process itself. The CR is a precision measure representing the unit scale value below which the absolute difference between two repeated measurements may be expected to lie with a probability of 95%. In our case, we observed a smaller CR for the oxCCO signal (CR = 0.248/0.157) compared with the hemodynamic signals (Table 1) most likely because its *in vivo* concentration is ∼10% that of hemoglobin. Therefore, the CRs of the metabolic and the hemodynamic signals may not be directly comparable.

The CV as another measure of dispersion, however, is expressed as a percentage, thus allowing for a direct comparison between the metabolic and the hemodynamic signals. The CV also showed a relatively small value for the oxCCO signal (CV = 4.432%/3.694%) compared with the hemodynamic signals (Table 1) suggesting that the degree of variation between sessions was smaller. Notably, the CV of the peripheral measures

**Table 1** Reliability, agreement, and repeatability. ICCs and Bland–Altman measures, i.e., the MD with lower and upper LoA, the CR and the CV, between sessions for both the hypo- and hypercapnia challenge. See Figs. 5 and 6 for illustration.

| | | | $\Delta PetCO_2$ | $\Delta SpO_2$ | ΔoxCCO | ΔTOI | $\Delta HbO_2$ | ΔHHb |
|---|---|---|---|---|---|---|---|---|
| Hypocapnia | Reliability | ICC | 0.793 | 0.667 | 0.827 | 0.574 | 0.841 | 0.804 |
| | | Upper 95% CI | 0.944 | 0.905 | 0.954 | 0.874 | 0.958 | 0.948 |
| | | Lower 95% CI | 0.366 | 0.109 | 0.449 | −0.043 | 0.483 | 0.392 |
| | | *p*-value | 0.002 | 0.012 | 0.001 | 0.032 | 0.001 | 0.001 |
| | Agreement | MD | −3.860 | 0.015 | 0.062 | −0.709 | −0.366 | 0.127 |
| | | Upper 95% LoA | −0.633 | 0.053 | 0.310 | 1.762 | 0.128 | 0.556 |
| | | Lower 95% LoA | −7.088 | −0.023 | −0.185 | −3.180 | −0.860 | −0.302 |
| | Repeatability | CR | 3.228 | 0.038 | 0.248 | 2.471 | 0.494 | 0.429 |
| | | CV % | 0.814 | 3.455 | 4.432 | 1.033 | 2.003 | 1.320 |
| Hypercapnia | Reliability | ICC | 0.687 | 0.833 | 0.913 | 0.502 | 0.805 | 0.707 |
| | | Upper 95% CI | 0.912 | 0.956 | 0.978 | 0.848 | 0.948 | 0.918 |
| | | Lower 95% CI | 0.146 | 0.463 | 0.690 | −0.143 | 0.393 | 0.182 |
| | | *p*-value | 0.010 | 0.001 | 0.000 | 0.058 | 0.001 | 0.008 |
| | Agreement | MD | 0.597 | 0.008 | −0.004 | −0.065 | 0.275 | −0.131 |
| | | Upper 95% LoA | 2.910 | 0.036 | 0.154 | 2.042 | 0.918 | 0.301 |
| | | Lower 95% LoA | −1.717 | −0.021 | −0.161 | −2.173 | −0.369 | −0.562 |
| | Repeatability | CR | 2.314 | 0.029 | 0.157 | 2.108 | 0.644 | 0.431 |
| | | CV % | 0.648 | 22.016 | 3.694 | 5.708 | 11.144 | 2.658 |

($PetCO_2$, $SpO_2$) cannot be compared with those of the fNIRS signals because of the different units.

## 5 Discussion

Cortical CCO measurements derived from fNIRS can yield crucial information about cerebral mitochondrial metabolism. As its first demonstration in 1977,[42] recent developments in instrumentation and analytical methods used to resolve the oxCCO signal[16,43,44] have led to several clinical applications of the measurement as indicated by a substantial literature regarding measures of CCO in humans (for review see Ref. 14). With the potential ability to use the oxCCO signal as a marker of mitochondrial health, this signal is important for our understanding of the human brain in health and disease.

The present test–retest study showed evidence for the reliability of the mitochondrial metabolic signal and compared it with those of the hemodynamic fNIRS signals in human brain. Reliability of the hemodynamic measurements has been previously shown to be excellent in healthy adults (ICC = 0.80 to 0.84),[6–8] in line with our results (ICC = 0.707 to 0.841). Reliability of the metabolic oxCCO signal, in contrast, has not been published previously and we found it to be excellent as well (ICC = 0.827 to 0.913) (Figs. 5 and 6, Table 1). Together, these findings suggest that the oxCCO signal can be reliably measured under conditions of respiratory challenges to be implemented effortlessly in both research and clinical settings.

Reliability depends on several aspects that should be kept in mind when interpreting our results. Regarding instrumentation, the present study utilized an NIRO 300 instrument (Hamamatsu Photonics), an early-generation instrument built ∼20 years ago. The NIRO 300 instrument has overall been shown to produce valid measurements of the oxCCO signal.[20,45–53] However, it belongs to those early-generation instruments that used only four discrete wavelengths (775, 810, 850, and 910 nm, respectively) to assess both the metabolic and hemodynamic signals. These wavelengths are in relatively good agreement with the optimal wavelengths reported for CCO measures.[43] Nonetheless, this technology has been superseded by systems using broadband spectroscopy covering a near-infrared wavelength resolution from ∼780 to 900 nm that is thought to obtain a more robust oxCCO signal.[16,24,43,54] There are also novel signal algorithms based on diffusion approximation, which have been suggested as an alternative to the modified Beer–Lambert's law used in the present work for the deconvolution of oxCCO.[54,55] Such algorithms are thought to avoid the possibility of cross talk between the hemodynamic and metabolic changes that might occur when using the MBLL algorithm.[56,57] It is thus possible that some of the drawbacks of the NIRO 300 instrumentation, such as low wavelength resolution and possible cross talk, might have affected the reliability of the present data. The exact evaluation of the corresponding instrumental behavior would, however, go beyond the scope of the present work. Using

technology reliability of the metabolic signal may even improve. This consideration has been accounted for in the ICC calculation (i.e., by choosing the corresponding type two-way mixed model with single measures).

Regarding timing, the test–retest data were collected in two sessions separated by one week. It may be assumed that, within this time period, the intervening respiratory challenges did not change the ability to induce hypo- and hypercapnia. Participants were further asked to maintain their breathing patterns between sessions such as the strength or depth of breath during hyperventilation. Thus, test–retest reliability should have not been compromised by timing. This assumption was supported by the good reliability observed for the respiratory parameters ($PetCO_2$ ICC = 0.793/0.687, $SpO_2$ ICC = 0.667/0.833) reflecting consistency of the administered respiratory challenges (Figs. 5 and 6, Table 1). Longer time spans, in contrast, such as a year or more, may affect reliability or circumstances where individuals experience changes in pulmonary, metabolic, or vascular systems, reflecting a change in signal and its measurement.

Regarding probe positioning, the test–retest data were collected from the same cortical areas, repositioned by the same experimenter. The probe itself, however, consisted of only a small number of channels. Nonetheless, this aspect was considered of minor relevance for the purpose of test–retesting as the spatial distribution of oxCCO changes in human brain requires further investigation before being quantified.[44,58] In other words, we expected to deal with global (nonlocalized) changes across the whole prefrontal cortex suggested to be unchanged between sessions. Considering cerebral pathological changes, in contrast, would unlikely be expected to have a uniform distribution across the brain, such as in the case of known brain disease or brain injury and may then require regional (localized) measures of oxCCO. Signal alterations in such cases may be smaller than those tested in this study and may require measurements of greater reliability.

## 6 Conclusion

Taken together, we found robust reliability of both the metabolic oxCCO signal and the hemodynamic signals derived from fNIRS in the human brain. These findings suggest that the oxCCO signal can be reliably measured under conditions of respiratory challenges to be implemented effortlessly in both research and clinical settings.

### Disclosures

The authors declare no conflicts of interest.

### Acknowledgments

The work was funded by a Janssen Fellowship in Translational Neuroscience at Columbia University, New York, awarded to LH.

### References

1. H. Obrig and A. Villringer, "Beyond the visible—imaging the human brain with light," *J. Cereb. Blood Flow Metab.* **23**(1), 1–18 (2003).
2. M. Ferrari and V. Quaresima, "A brief review on the history of human functional near-infrared spectroscopy (fNIRS) development and fields of application," *NeuroImage* **63**(2), 921–935 (2012).
3. M. Wolf, M. Ferrari, and V. Quaresima, "Progress of near-infrared spectroscopy and topography for brain and muscle clinical applications," *J. Biomed. Opt.* **12**(6), 062104 (2007).
4. M. Ferrari, L. Mottola, and V. Quaresima, "Principles, techniques, and limitations of near infrared spectroscopy," *Can. J. Appl. Physiol.* **29**(4), 463–487 (2004).
5. L. Li et al., "Tutorial on use of intraclass correlation coefficients for assessing intertest reliability and its application in functional near-infrared spectroscopy-based brain imaging," *J. Biomed. Opt.* **20**(5), 050801 (2015).
6. M. M. Plichta et al., "Event-related functional near-infrared spectroscopy (fNIRS): are the measurements reliable?" *NeuroImage* **31**(1), 116–124 (2006).
7. M. Plichta et al., "Event-related functional near-infrared spectroscopy (fNIRS) based on craniocerebral correlations: reproducibility of activation?" *Hum. Brain Mapp.* **28**(8), 733–741 (2007).
8. Y. Bhambhani et al., "Reliability of near-infrared spectroscopy measures of cerebral oxygenation and blood volume during handgrip exercise in nondisabled and traumatic brain-injured subjects," *J. Rehabil. Res. Dev.* **43**(7), 845–856 (2006).
9. H. Zhang et al., "Test–retest assessment of independent component analysis-derived resting-state functional connectivity based on functional near-infrared spectroscopy," *NeuroImage* **55**(2), 607–615 (2011).
10. H. Niu et al., "Test-retest reliability of graph metrics in functional brain networks: a resting-state fNIRS study," *PLoS One* **8**(9), e72425 (2013).
11. A. Blasi et al., "Test-retest reliability of functional near infrared spectroscopy in infants," *Neurophotonics* **1**(2), 025005 (2014).
12. B. Celie et al., "Reliability of near infrared spectroscopy (NIRS) for measuring forearm oxygenation during incremental handgrip exercise," *Eur. J. Appl. Physiol.* **112**(6), 2369–2374 (2012).
13. V. M. Niemeijer et al., "Test–retest reliability of skeletal muscle oxygenation measurements during submaximal cycling exercise in patients with chronic heart failure," *Clin. Physiol. Funct. Imaging* **37**(1), 68–78 (2017).
14. G. Bale, C. Elwell, and I. Tachtsidis, "From Jöbsis to the present day: a review of clinical near-infrared spectroscopy measurements of cerebral cytochrome-c-oxidase," *J. Biomed. Opt.* **21**(9), 091307 (2016).
15. O.-M. H. Richter and B. Ludwig, "Cytochrome-c-oxidase—structure, function, and physiology of a redox-driven molecular machine," *Rev. Physiol. Biochem. Pharmacol.* **147**, 47–74 (2003).
16. G. Bale et al., "A new broadband near-infrared spectroscopy system for in-vivo measurements of cerebral cytochrome-c-oxidase changes in neonatal brain injury," *Biomed. Opt. Express* **5**(10), 3450–3466 (2014).
17. I. de Roever et al., "Functional NIRS measurement of cytochrome-c-oxidase demonstrates a more brain-specific marker of frontal lobe activation compared to the haemoglobins," in *Oxygen Transport to Tissue*, H. J. Halpern et al., Eds., Vol. **XXXIX**, pp. 141–147, Springer International Publishing, Cham (2017).
18. I. de Roever et al., "Cytochrome-c-oxidase exhibits higher brain-specificity than haemoglobin in functional activation," in *Biomedical Optics*, OSA (2016).
19. C. Kolyva et al., "Cytochrome-c-oxidase response to changes in cerebral oxygen delivery in the adult brain shows higher brain-specificity than haemoglobin," *Neuroimage* **85**(Pt 1), 234–244 (2014).
20. I. Tachtsidis et al., "Relationship between brain tissue haemodynamics, oxygenation and metabolism in the healthy human adult brain during hyperoxia and hypercapnea," *Oxygen Transp. Tissue* **645**, 315–320 (2009).
21. D. Highton et al., "Analysis of slow wave oscillations in cerebral haemodynamics and metabolism following subarachnoid haemorrhage," *Adv. Exp. Med. Biol.* **812**, 195–201 (2014).
22. C. Kolyva et al., "Dependence on NIRS source-detector spacing of cytochrome-c-oxidase response to hypoxia and hypercapnia in the adult brain," *Adv. Exp. Med. Biol.* **789**, 353–359 (2013).
23. A. Ghosh et al., "Reduction of cytochrome-c-oxidase during vasovagal hypoxia-ischemia in human adult brain: a case study," *Adv. Exp. Med. Biol.* **789**, 21–27 (2013).
24. A. Bainbridge et al., "Brain mitochondrial oxidative metabolism during and after cerebral hypoxia–ischemia studied by simultaneous phosphorus magnetic-resonance and broadband near-infrared spectroscopy," *Multimodal Data Fusion* **102**(Part 1), 173–183 (2014).
25. A. Ghosh et al., "Hyperoxia results in increased aerobic metabolism following acute brain injury," *J. Cereb. Blood Flow Metab.* **37**(8), 2910–2920 (2017).

26. I. Tachtsidis et al., "Analysis of the changes in the oxidation of brain tissue cytochrome-c-oxidase in traumatic brain injury patients during hypercapnoea: a broadband NIRS study," *Adv. Exp. Med. Biol.* **701**, 9–14 (2011).
27. M. Banaji et al., "Modelling of mitochondrial oxygen consumption and NIRS detection of cytochrome oxidase redox state," *Adv. Exp. Med. Biol.* **662**(Part 2), 285–291 (2010).
28. R. Nosrati et al., "Event-related changes of the prefrontal cortex oxygen delivery and metabolism during driving measured by hyperspectral fNIRS," *Biomed. Opt. Express* **7**(4), 1323–1335 (2016).
29. L. Holper, F. Scholkmann, and E. Seifritz, "Time–frequency dynamics of the sum of intra- and extracerebral hemodynamic functional connectivity during resting-state and respiratory challenges assessed by multimodal functional near-infrared spectroscopy," *NeuroImage* **120**, 481–492 (2015).
30. D. Delpy et al., "Estimation of optical pathlength through tissue from direct time of flight measurement," *Phys. Med. Biol.* **33**(12), 1433–1442 (1988).
31. M. S. Patterson, B. Chance, and B. C. Wilson, "Time resolved reflectance and transmittance for the noninvasive measurement of tissue optical properties," *Appl. Opt.* **28**(12), 2331–2336 (1989).
32. S. Matcher et al., "Absolute quantification methods in tissue near-infrared spectroscopy," *Proc SPIE* **2389**, 486–495 (1995).
33. H. Jaspers, "The ten-twenty electrode system of the International Federation," *Electroencephalogr. Clin. Neurophysiol.* **10**, 371–375 (1958).
34. T. Huppert et al., "HomER: a review of time-series analysis methods for near-infrared spectroscopy of the brain," *Appl. Opt.* **48**(10), D280–D298 (2009).
35. P. Shrout and J. Fleiss, "Intraclass correlations: uses in assessing rater reliability," *Psychol. Bull.* **86**(2), 420–428 (1979).
36. D. Cicchetti, "Guidelines, criteria, and rules of thumb for evaluating normed and standardized assessment instruments in psychology," *Psychol. Assess.* **6**(4), 284–290 (1994).
37. J. Bland and D. Altman, "Statistical methods for assessing agreement between two methods of clinical measurement," *Lancet* **327**, 307–310 (1986).
38. J. M. Bland and D. G. Altman, "Comparing methods of measurement: why plotting difference against standard method is misleading," *Lancet* **346**(8982), 1085–1087 (1995).
39. J. M. Bland and D. G. Altman, "Measuring agreement in method comparison studies," *Stat. Methods Med. Res.* **8**(2), 135–160 (1999).
40. J. Bartlett and C. Frost, "Reliability, repeatability and reproducibility: analysis of measurement errors in continuous variables," *Ultrasound Obstet. Gynecol.* **31**, 466–475 (2008).
41. G. Rankin and M. Stokes, "Reliability of assessment tools in rehabilitation: an illustration of appropriate statistical analyses," *Clin. Rehabil.* **12**(3), 187–199 (1998).
42. F. Jöbsis, "Noninvasive, infrared monitoring of cerebral and myocardial oxygen sufficiency and circulatory parameters," *Science* **198**(4323), 1264–1267 (1977).
43. D. Arifler et al., "Optimal wavelength combinations for near-infrared spectroscopic monitoring of changes in brain tissue hemoglobin and cytochrome-c-oxidase concentrations," *Biomed. Opt. Express* **6**(3), 933–947 (2015).
44. P. Phan et al., "A new multichannel broadband near infrared spectroscopy system to measure the spatial distribution of cytochrome-c-oxidase and tissue oxygenation," in *Biomedical Optics*, OSA (2016).
45. P. Zaramella et al., "Brain auditory activation measured by near-infrared spectroscopy (NIRS) in neonates," *Pediatr. Res.* **49**(2), 213–219 (2001).
46. A. Azakie et al., "Cerebral oxygen balance is impaired during repair of aortic coarctation in infants and children," *J. Thorac. Cardiovasc. Surg.* **130**(3), 830–836 (2005).
47. N. Nagdyman et al., "Cerebral oxygenation measured by near-infrared spectroscopy during circulatory arrest and cardiopulmonary resuscitation," *Br. J. Anaesth.* **91**(3), 438–442 (2003).
48. C. Dani et al., "Brain hemodynamic changes in preterm infants after maintenance dose caffeine and aminophylline treatment," *Neonatology* **78**(1), 27–32 (2000).
49. A. McGown et al., "Measurement of changes in cytochrome oxidase redox state during obstructive sleep apnea using near-infrared spectroscopy," *Sleep* **26**(6), 710–716 (2003).
50. E. McNeill et al., "Cerebral oxygenation during defibrillator threshold testing of implantable cardioverter defibrillators," *Pacing Clin. Electrophysiol.* **28**(6), 528–533 (2005).
51. I. Tachtsidis et al., "Changes in cerebral total haemoglobin volume and cytochrome oxidase redox state during deep apnoeas in patients with obstructive sleep apnoea," in *Biomedical Topical Meeting*, p. WF6, Optical Society of America (2004).
52. I. Tachtsidis et al., "Investigation of in vivo measurement of cerebral cytochrome-c-oxidase redox changes using near-infrared spectroscopy in patients with orthostatic hypotension," *Physiol. Meas.* **28**(2), 199–211 (2007).
53. N. Nagdyman et al., "Comparison between cerebral tissue oxygenation index measured by near-infrared spectroscopy and venous jugular bulb saturation in children," *Intensive Care Med.* **31**(6), 846–850 (2005).
54. R. Nosrati et al., "Cerebral hemodynamics and metabolism during cardiac arrest and cardiopulmonary resuscitation using hyperspectral near infrared spectroscopy," *Circ. J.* **81**(6), 879–887 (2017).
55. A. V. Patil et al., "Experimental investigation of NIRS spatial sensitivity," *Biomed. Opt. Express* **2**(6), 1478–1493 (2011).
56. C. E. Cooper and R. Springett, "Measurement of cytochrome oxidase and mitochondrial energetics by near-infrared spectroscopy," *Philos. Trans. R. Soc. B Biol. Sci.* **352**(1354), 669–676 (1997).
57. Y. Kakihana et al., "Re-evaluation of the reliability of cytochrome oxidase—signal study of cardiopulmonary bypass," in *Oxygen Transport to Tissue XXV*, Advances in Experimental Medicine and Biology, M. Thorniley, D. K. Harrison, and P. E. James, Eds., Vol. **540**, Springer, Boston, Massachusetts (2003).
58. P. Phan et al., "Spatial distribution of changes in oxidised cytochrome-c-oxidase during visual stimulation using broadband near infrared spectroscopy imaging," *Adv. Exp. Med. Biol.* **923**, 195–201 (2016).



**Lisa Holper** received her MD degree from the University Medicine Berlin and has done her residency at the Department of Psychiatry, Psychotherapy, and Psychosomatics, Hospital of Psychiatry Zurich, University Zurich. Currently, she is working as a research fellow at the Columbia University and New York State Psychiatric Institute. She has published and contributed to over 30 papers addressing human research in healthy and psychiatric populations particularly in the field of optical brain imaging.

**J. John Mann** is the Paul Janssen professor of translational neuroscience and vice chair for research in the Department of Psychiatry at Columbia University. His research employs functional brain imaging, neurochemistry, and molecular genetics to probe the causes of depression and suicide. He has published 458 papers and edited 10 books on the subjects of the biology and treatment of mood disorders, suicidal behavior, and other psychiatric disorders.